

Article

An O-Demethylation Metabolite of Rabeprazole Sulfide by *Cunninghamella blakesleeana* 3.970 Biotransformation

Ming Song¹, Hongxiang Zhu², Jian Wang³ , Weizhuo Xu^{2,*}  and Wei Xu^{2,*}¹ School of Functional Food and Wine, Shenyang Pharmaceutical University, Shenyang 110016, China² School of Life Sciences and Biopharmaceuticals, Shenyang Pharmaceutical University, Shenyang 110016, China³ School of Pharmaceutical Engineering, Shenyang Pharmaceutical University, Shenyang 110016, China

* Correspondence: weizhuo.xu@syphu.edu.cn (W.X.); shxuwei8720@163.com (W.X.); Tel./Fax: +86-024-43520301 (Weizhuo Xu); Tel.: +86-024-43520307 (Wei Xu)

Abstract: To explore the potential metabolites from rabeprazole sulfide, seven strains of filamentous fungi were screened for their biotransformation abilities. Among these strains, *Cunninghamella blakesleeana* 3.970 exhibited the best result. Four different culture media were screened in order to identify the most optimal for subsequent research. Single factors such as the initial pH of culture media, culture time, inoculation volume, and media volume were individually investigated to provide the optimum biotransformation conditions. Then, an orthogonal optimization process using a five-factor, four-level $L_{16}(4^5)$ experiment was designed and performed. Finally, when the substrate concentration is 3 g/L, one major metabolite was detected with a transformation rate of 72.4%. Isolated by semipreparative HPLC, this metabolite was further detected by ESI-MS and NMR. The final data analysis indicated that the metabolite is O-demethylation rabeprazole sulfide.

Keywords: rabeprazole; sulfide; biotransformation; *Cunninghamella blakesleeana* 3.970; O-demethylation rabeprazole sulfide



Citation: Song, M.; Zhu, H.; Wang, J.; Xu, W.; Xu, W. An O-Demethylation Metabolite of Rabeprazole Sulfide by *Cunninghamella blakesleeana* 3.970 Biotransformation. *Catalysts* **2023**, *13*, 15. <https://doi.org/10.3390/catal13010015>

Academic Editors: Zhilong Wang and Tao Pan

Received: 14 November 2022

Revised: 16 December 2022

Accepted: 17 December 2022

Published: 22 December 2022



Copyright: © 2022 by the authors. Licensee MDPI, Basel, Switzerland. This article is an open access article distributed under the terms and conditions of the Creative Commons Attribution (CC BY) license (<https://creativecommons.org/licenses/by/4.0/>).

1. Introduction

Rabeprazole is a kind of proton pump inhibitor, which has been widely used in the treatment of gastric acid secretion, and can also be applied to eradicate *Helicobacter pylori* [1]. As a benzimidazole derivative, rabeprazole has a heterocyclic molecule consisting of a pyridine and benzimidazole moiety linked by a methylsulfinyl group. This general structure guarantees the similar pharmacological properties of other proton pump inhibitors. Rabeprazole sulfide (rabeprazole thioether) is an essential intermediate for the production of rabeprazole [2,3]. Meanwhile, sulfide is also one of the metabolites produced by the rabeprazole metabolites in vivo [4–8].

Rabeprazole sulfide is an important imidazole compound, which is not only a precursor of rabeprazole synthesis, but is also one of the main metabolites of rabeprazole in vivo. As the primary metabolite of rabeprazole, rabeprazole sulfide can undergo further metabolic reactions such as demethylation and sulfuric acid binding. These demethylated metabolites often have pharmacological activity. Pharmacologically active metabolites can contribute significantly to the overall therapeutic and adverse effects of drugs. Therefore, to fully understand the mechanism of action of drugs, it is important to recognize the role of active metabolites [9–12].

Some microorganisms, especially the fungi belonging to *Cunninghamella* species, possess cytochrome P-450 mono-oxygenase systems analogous to those in mammals [13]. Hence, microbial transformation has been proposed as a complementary in vitro model for mammalian drug metabolism. *Cunninghamella* is a genus of fungi in the family *Cunninghamellaceae*, which has been implemented for in vitro biotransformations for a long time [14–20]. Various reaction types have been reported for these kinds of fungi. Previous studies have

demonstrated their hydroxylation [21–24], epoxidation [25–27], amination [28], demethylation [29], and oxidation from sulfide to sulfoxide, which is usually the final step for the production of prazole-type molecules [30–32].

Demethylated metabolites often have some unexpected pharmacological effects. Metamizole (dipyrone) is an analgesic with antipyretic and spasmolytic properties, which has been in use for almost 100 years. The primary metabolite of metamizole, 4-methylaminoantipyrine, can be *N*-demethylated to 4-aminoantipyrine. 4-aminoantipyrine plays a role as a non-steroidal anti-inflammatory drug, a non-narcotic analgesic, an antirheumatic drug, a peripheral nervous system drug, and an EC 1.14.99.1 (prostaglandin-endoperoxide synthase) inhibitor. It is used as a reagent for biochemical reactions, such as the production of peroxides or phenols [33,34]. Papaverine plays a role as a vasodilator agent and an anti-spasmodic drug. The metabolism of papaverine with *Cunninghamella echinulate* results in *O*-demethylation. 4'-*O*-demethylated papaverine, 3'-*O*-demethylated papaverine, and 6-*O*-demethylated papaverine have been isolated. In silico docking studies of these metabolites using crystals of human phosphodiesterase 10a (hPDE10a) revealed that the compounds 4'-*O*-demethylated papaverine and 6-*O*-demethylated papaverine possess better docking scores and binding poses with favorable interactions than the native ligand papaverine [35].

In this report, seven strains of filamentous fungi are investigated for their ability to metabolize the rabeprazole sulfide, in order to explore the reaction types of the whole cell transformation. Instead of hunting for the sulfoxide metabolites obtained, an *O*-demethyl rabeprazole sulfide, a new compound with potential pharmacological activity, was finally isolated and identified (Figure 1), which is the first report of the *O*-demethyl reaction in rabeprazole sulfide to date.

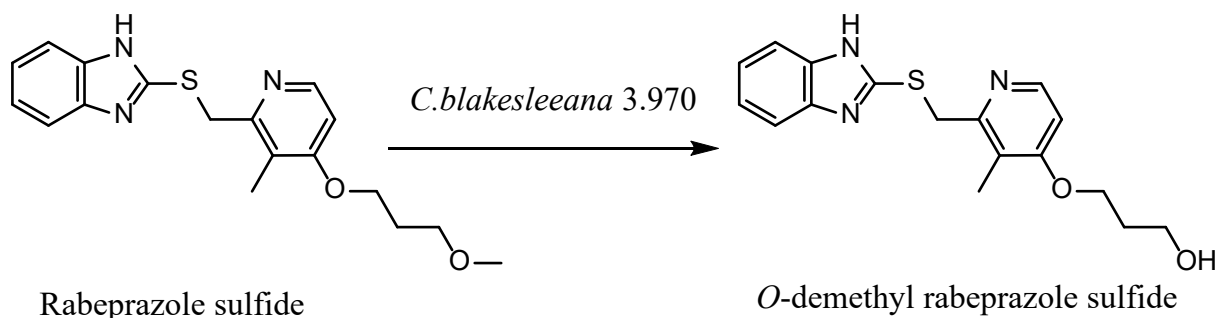


Figure 1. Rabeprazole sulfide and its *O*-demethyl metabolite obtained by the biotransformation of *Cunninghamella blakesleeana* 3.970.

2. Results and Discussion

2.1. Whole-Cell Biotransformation Results of Rabeprazole Sulfide

Among the seven strains, *Cunninghamella elegans* 3.910, *Cunninghamella echinulate* 3.967, *Cunninghamella blakesleeana* 3.970, and *Absidia coerulea* 41,050 displayed different transformation results for rabeprazole sulfide. *Cunninghamella elegans* 3.910 and *Cunninghamella blakesleeana* 3.970 demonstrated a rather significant major metabolite spectrum, whereas *Gibberella fujiluroi* 40,272, *Gibberella* sp. 2498, and *Caldariomyces fumago* 16,373 did not indicate any positive transformation result. According to the transformation TLC results (Figure 2), the fungus *Cunninghamella blakesleeana* 3.970 converted rabeprazole sulfide to rabeprazole and another, novel compound, and the conversion rate of this new compound was high. Therefore, *Cunninghamella blakesleeana* 3.970 was selected for further study.

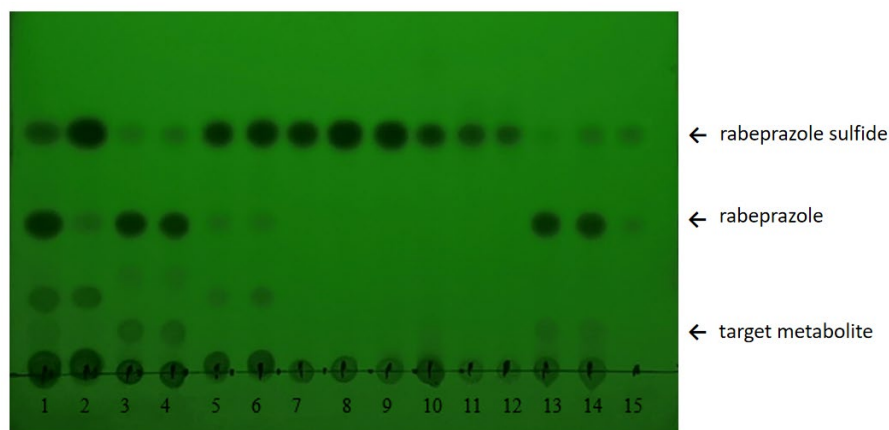


Figure 2. TLC screening results for seven strains of filamentous fungi for rabeprazole sulfide. Lanes 1 and 2, *Cunninghamella elegans* 3.910, 3 and 4, *Cunninghamella echinulata* 3.967, 5 and 6, *Absidia coerulea* 41,050, 7 and 8, *Gibberella* sp. 2498, 9 and 10, *Caldariomyces fumago* 16,373, 11 and 12, *Gibberella fujiluroi* 40,272, 13 and 14, *Cunninghamella blakesleeana* 3.970, and 15, standard mixture of rabeprazole sulfide and rabeprazole.

2.2. Optimization of Transformation Media

In order to obtain the transformation products of rabeprazole sulfide, four microbial media were screened. The evaluation criteria were set according to both the growth of the strain and the HPLC detection diagram for the transformation solution. According to Figure S1, fewer mycelium balls were observed in medium 1 and medium 2, and the color of the mycelium ball was a little pink in medium 3, which is not its usual appearance. Only in medium 4 were the numbers of the mycelium balls ambient and the growth of mycelium good.

It can be seen from the HPLC results in Figure S1 that under the same substrate concentration, the ability of transformation media 1, 2, and 3 to transform rabeprazole sulfide is low, and the transformation products are relatively miscellaneous. However, transformation medium 4 had a higher ability to transform rabeprazole sulfide, and only one transformation product was produced. Therefore, based on the results in Figures S1 and S2, medium 4 was selected as the medium for subsequent fermentation.

2.3. Single-Factor Evaluation for Rabeprazole Sulfide Biotransformation

2.3.1. Standard Curve of Rabeprazole Sulfide

Figure 3 indicates that the linear correlation coefficient $R^2 = 0.9995$ and the correlation equation $y = 18,285x + 66.794$ for the concentration and peak area of rabeprazole sulfide, with a good linear correlation. This standard curve can be used to calculate the conversion rate of rabeprazole sulfide.

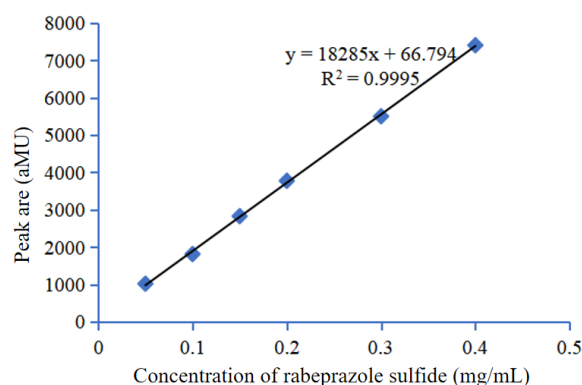


Figure 3. Standard curve of rabeprazole sulfide.

2.3.2. Evaluation of Culture Time

The culture duration of whole-cell catalysis has an important effect on the reaction. If the reaction time is too short, the reaction may not be accomplished. If the reaction time is too long, product inhibition may occur and the total transformation rate may decrease. In this section, we investigate the effect of conversion time on the production of metabolites; the results are shown in Figure 4.

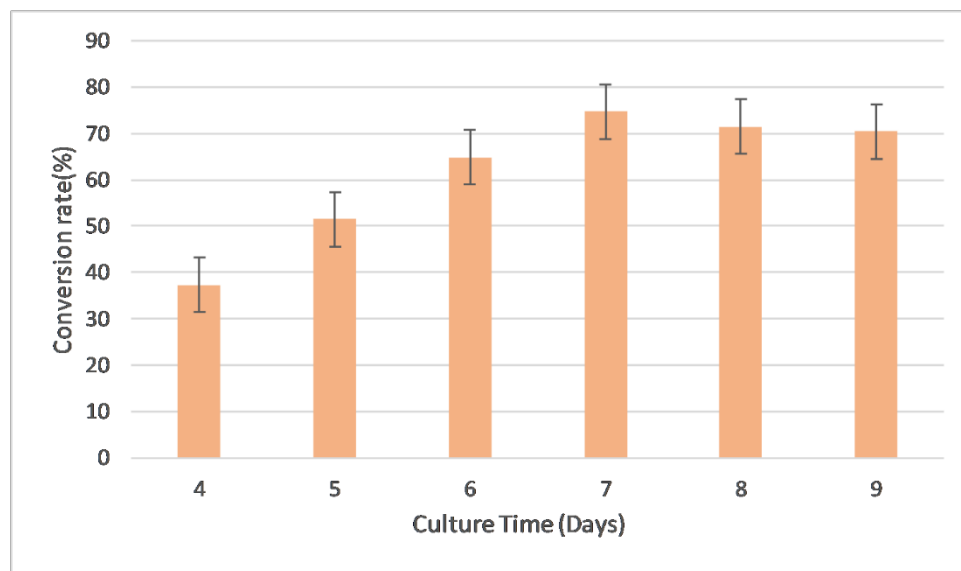


Figure 4. Effects of culture time on metabolite conversion rate (initial pH = 6.5, media volume 50 mL, inoculation volume 10%, substrate concentration 1 mg/mL).

When the transformation was performed at 28 °C, 200 rpm, it could be seen that the culture time ranged between 6 and 9 days. A culture time of 7 days resulted in the optimal conversion rate of 74.71%.

2.3.3. Evaluation of Initial pH

The initial pH of the media is vital for strain growth and transformation. A pH that is too low or high will cause the strains to undergo non-ambient growth and affect their metabolism capability. This is why different strains desire specific initial pH values in their media. In this section, a pH range of 5.5 to 8.0 was selected for the investigation. From Figure 5, it can be seen that both the acid and alkaline conditions are not fit for biotransformation, so the best initial pH is set to 6.0.

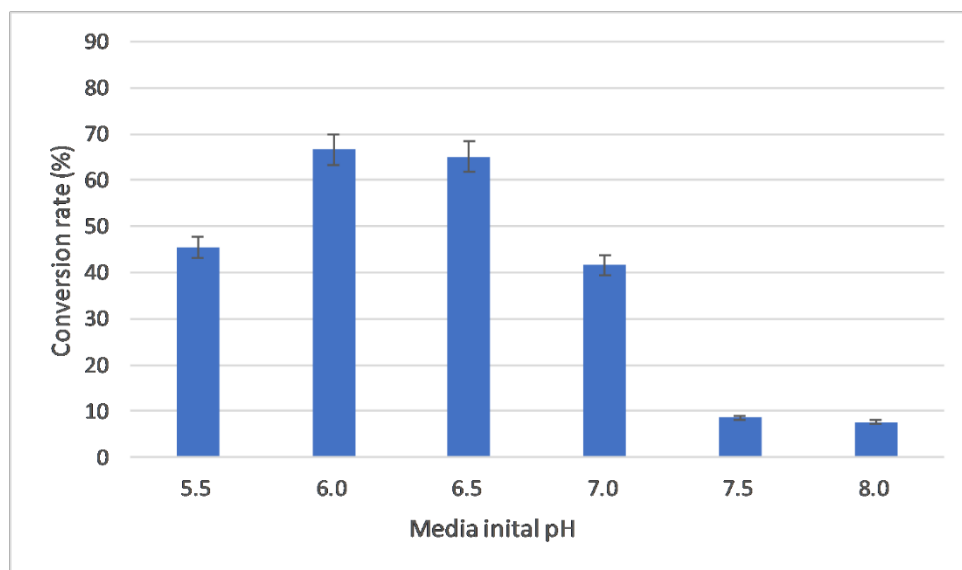


Figure 5. Effects of the initial pH of the media on the metabolite conversion rate (culture time 5 d, media volume 50 mL, inoculation volume 10%, substrate concentration 1 mg/mL).

2.3.4. Evaluation of Media Volume

The media volume is crucial for the transformation effects, which are related to the dissolved oxygen when the conical flask volume is constant. Media volumes from 30 mL to 120 mL were selected for the investigation. From Figure 6, it can be seen that a media volume of 50 mL displayed the best transformation effect.

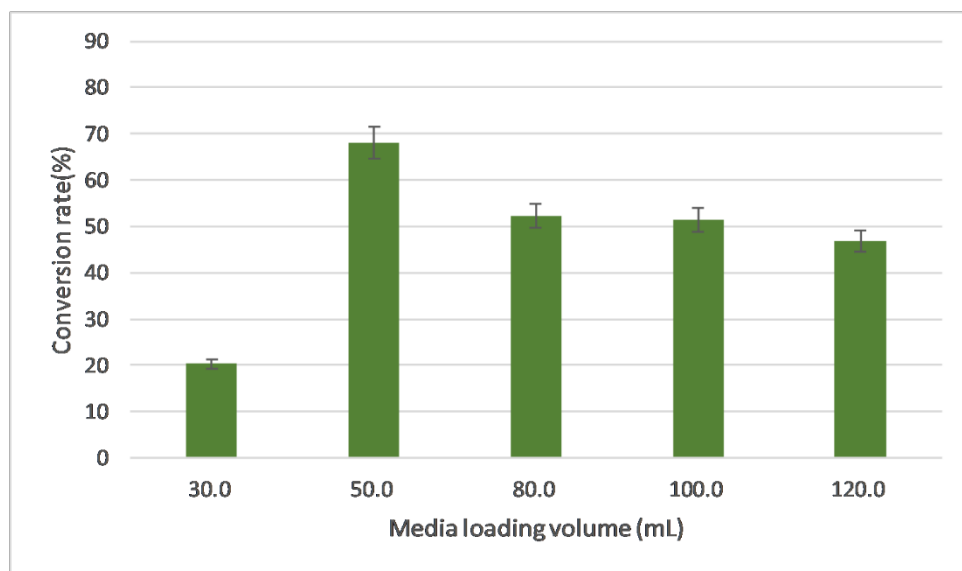


Figure 6. Effects of media volume on metabolite conversion rate (initial pH = 6.5, culture time 5 d, inoculation volume 10%, substrate concentration 1 mg/mL).

2.3.5. Evaluation of Inoculation Volume

Inoculation volume is a critical factor for the biotransformation process. If the inoculation volume is high, the strains will grow to the exponential phase too early and the nutrients will be depleted quickly, such that the enzymes in the strains may not sufficiently be induced and expressed, and the biotransformation may not be adequate. If the inoculation volume is low, the strains may take too long a time to grow and induce enzymes, which

may decrease their metabolism capabilities. Based our previous experiences, inoculation volumes ranging from 6% to 14% were selected for the investigation.

From Figure 7, it can be seen that an inoculation volume of 10% is the best for biotransformation.

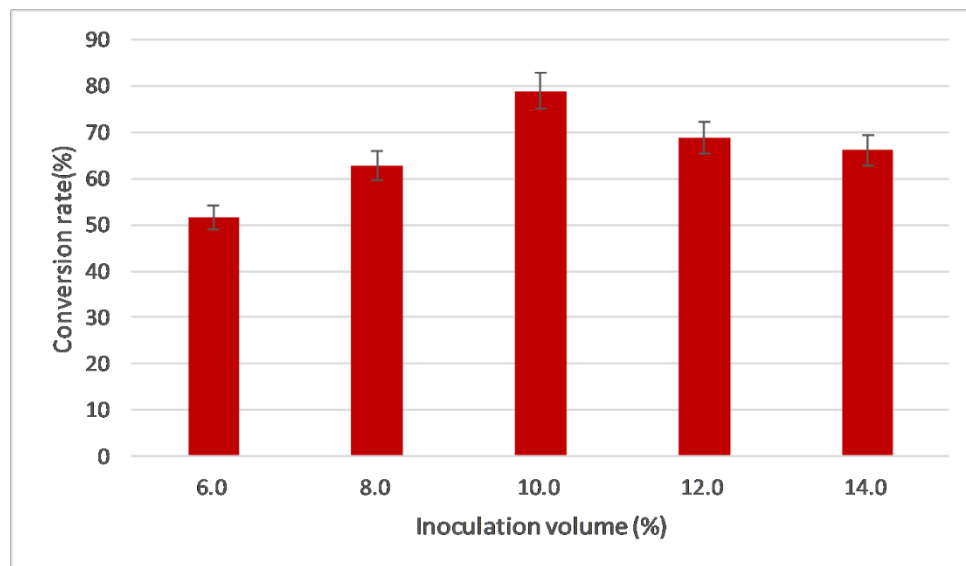


Figure 7. Effects of inoculation volume on metabolite conversion rate (initial pH = 6.5, culture time 5 d, media volume 50 mL, substrate concentration 1 mg/mL).

2.3.6. Evaluation of Substrate Concentration

In this study, rabeprazole sulfide is not a natural substrate, which may cause severe inhibition and toxic effects for the strains. Hence, a proper substrate concentration is essential for successful biotransformation. A substrate concentration range from 1 mg/mL to 5 mg/mL was set for the investigation.

From Figure 8, it can be seen from the decreasing conversion rate tendency that 1 mg/mL substrate concentration is the best for biotransformation.

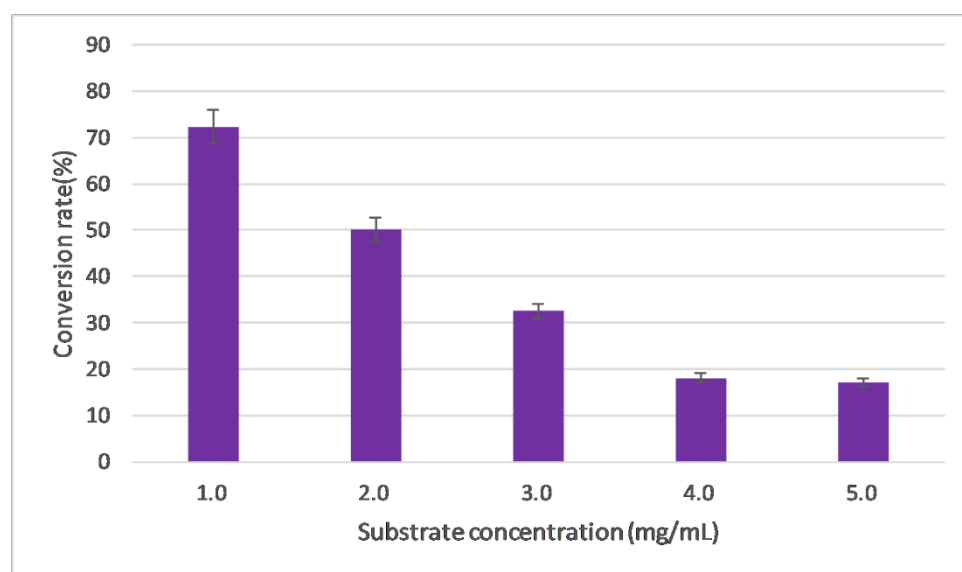


Figure 8. Effects of substrate concentration on metabolite conversion rate (initial pH = 6.5, culture time 5 d, media volume 50 mL, substrate concentration 1 mg/mL).

2.4. Orthogonal Optimization

According to the above single-factor investigation results, a 5-factor, 4-level, orthogonal $L_{16}(4^5)$ optimization process was designed, as shown in Table 1.

Table 1. Orthogonal experimental factors and level assignments.

Factor Level	A/Culture Time (Days)	B/Inoculation Volume (%)	C/Media Volume (mL)	D/Media Starting pH	E/Substrate Concentration (g/L)
1	5	8	30	5.5	1
2	6	10	50	6.0	2
3	7	12	80	6.5	3
4	8	14	100	7.0	4

After the design and execution of the experiments, it could be seen that the strength of impact of the various factors on biotransformation was in the order $D > B > E > C > A$, i.e., the most significant influence was that of the initial pH value of the media, as shown in Table 2. When the range analysis was performed, it was found that the best combination was $D_2B_1E_3C_4A_4$, so an initial pH of 6.0, inoculation volume of 8%, substrate concentration of 3 mg/mL, media volume of 100 mL, and culture time of 8 days were the best values. These values are consistent between the best results from the orthogonal design and those from the No.13 experimental group (total 16 groups), with a conversion rate of 72.4%. This is almost a double increase in the conversion rate compared with the unoptimized results.

Table 2. Orthogonal experimental results and analysis.

Factors Experiment No.	A	B	C	D	E	Conversion Rate
1	1	1	1	1	1	0.352
2	1	2	2	2	2	0.315
3	1	3	3	3	3	0.348
4	1	4	4	4	4	0.201
5	2	1	2	3	4	0.213
6	2	2	1	4	3	0.124
7	2	3	4	1	2	0.336
8	2	4	3	2	1	0.566
9	3	1	3	4	2	0.347
10	3	2	4	3	1	0.171
11	3	3	1	2	4	0.135
12	3	4	2	1	3	0.343
13	4	1	4	2	3	0.724
14	4	2	3	1	4	0.053
15	4	3	2	4	1	0.094
16	4	4	1	2	3	0.033
K1	1.216	1.636	0.644	1.084	1.184	
K2	1.24	0.664	0.964	1.812	1.032	
K3	0.996	0.912	1.312	0.764	1.54	
K4	1.304	1.144	1.432	0.764	0.604	
k1	0.304	0.409	0.161	0.271	0.296	
k2	0.310	0.166	0.241	0.453	0.258	
k3	0.249	0.228	0.328	0.191	0.385	
k4	0.326	0.286	0.358	0.191	0.151	
$R_{(Range\ analysis)}$	0.084	0.243	0.197	0.244	0.234	
Best combination	A2	B1	C4	D2	E1	

2.5. Structure Identification for the Rabeprazole Sulfide Biotransformation

The isolated metabolite was resolved in DMSO for the MS and NMR analysis. According to the ESI-MS results, showing that the m/z $[M+H]^+$ is 330.25 (Figure S3) and the m/z

$[M-H]^-$ is 328.27 (Figure S4), it could be inferred that the target metabolite has a molecular weight of 329.12, which is only a Dalton loss of 14 compared with the original rabeprazole sulfide with a molecular weight of 343.44. Hence, the loss of a methyl group is assumed.

According to the comparison of the NMR data between the substrate and metabolite, it could be found that a methyl and a carbon signal are absent in the H spectrum and C spectrum. Combined with the MS and NOESY data (Figure S7) indicating a methyl loss, it can be concluded that the target metabolite is the *O*-dimethyl rabeprazole sulfide (Figure 1). The analysis is given below.

$^1\text{H-NMR}$ (600 MHz, $\text{DMSO-}d_6$) δH : 8.23 (1H, d, $J = 5.6$ Hz), 7.45 (2H, dd, $J_1 = 5.8$, $J_2 = 3.2$ Hz), 7.11 (2H, dd, $J_1 = 5.9$, $J_2 = 3.1$ Hz), 6.95 (1H, d, $J = 5.6$ Hz), 4.69 (2H, s), 4.12 (2H, t, $J = 6.2$ Hz), 3.58 (2H, t, $J = 6.2$ Hz), 2.21 (3H, s), 1.87–1.91 (2H, m).

$^{13}\text{C-NMR}$ (150 MHz, $\text{DMSO-}d_6$) δC : 163.27, 155.16, 150.90, 148.24, 121.73, 120.20, 106.78, 65.50, 57.56, 36.74, 32.31, 10.88.

3. Materials and Methods

3.1. Materials and Strains

Rabeprazole sulfide was synthesized in the Department of Pharmaceutical Engineering, Shenyang Pharmaceutical University. Methanol and acetonitrile were purchased from Concord Technology Co., Ltd. (Tianjin, China). Peptone and yeast extract were purchased from HopeBio Co., Ltd. (Qingdao, China). All other chemical reagents were purchased from Yuwang Chemical Co., Ltd. (Shenyang, China).

Cunninghamella blakesleeana 3.970 and *Cunninghamella elegans* 3.910 were stored in our lab reservoir. *Cunninghamella echinulata* 3.967, *Absidia coerulea* 41,050, *Gibberella fujiluroi* 40,272, *Gibberella* sp. 2498, and *Caldariomyces fumago* 16,373 were purchased from China Center of Industrial Culture Collection (CICC).

3.2. Media and Strain Cultivations

Slant and agar media consisted of potato (200 g), glucose (20 g), agar (20 g), and 1000 mL distilled water. Seed culture media consisted of potato starch (45 g), yeast extract (3 g), corn steep liquor (10 g), CaCO_3 (3 g), MgSO_4 (0.5 g), and FeSO_4 (0.05 g). Four kinds of biotransformation culture media ingredients are listed in Table 3. For all media, the pH was adjusted to 6.5 with 6 M HCl, autoclaved at 115 °C for 30 min, and cooled before use.

Table 3. Four different biotransformation media formulas.

Ingredients	No.1 (g)	No.2 (g)	No.3 (g)	No.4 (g)
Sucrose	30		15	
Yeast extracts	20	0.5		2
Corn steep liquor	5			
Peptone		0.5	5	5
Glucose		4	15	50
K_2HPO_4	16	0.5	1	4
KH_2PO_4	2			5
MgSO_4	0.5		0.5	0.2
FeSO_4	0.05		0.01	0.05
KCl		0.5	0.5	

Two loops of mycelium from a fresh growth slant were inoculated into the seed culture media and cultured at 28 °C, 200 rpm for 48 h. Then, 5 mL of seed culture was inoculated into the transformation media (50 mL in a 250 mL conical flask, rabeprazole sulfide as substrate) and cultured at 28 °C, 200 rpm for 5 days. Substrate controls were set without inoculating the fungi into the media and strain controls were set without adding the substrate into the media, with all other conditions remaining the same.

3.3. Thin-Layer Chromatography (TLC)

The biotransformation results of the fungal extracts were analyzed by TLC performed on a Merck Silica gel 60 F254 plate (Merck, Darmstadt, Germany) with ethyl acetate:methanol:ammonia water (90:9:1 *v/v/v*) as the mobile phase, and a UV detection wavelength of 254 nm. A mixture of rabeprazole sulfide and rabeprazole (10 mg) was dissolved in 100 mL of isopropyl alcohol used as a standard solution. For TLC detection, 10 μ L of standard solution and fungal extracts was spotted onto TLC plates.

3.4. Extraction of Metabolites and HPLC Detection

Biotransformation cultures were collected, ultrasonically treated for 30 min, and centrifugated at 3000 rpm for 10 min to retrieve the supernatant. Pellets were washed and extracted three times using ethyl acetate. The combined water phase and organic phase were extracted three times with an equal volume of ethyl acetate. The organic phase was then isolated and evaporated by reduced pressure distillation to obtain the raw metabolites. The raw metabolites were dissolved in methanol for further use.

The HPLC detection process for the metabolites was derived from the Pharmacopeia of the People's Republic of China (2020 Volume II) and optimized according to our practical work. For High-performance liquid chromatography (HPLC), a Shimadzu WondaSil C18 Superb (250 \times 4.6 mm \times 5 μ m) column (Shimadzu Corp., Kyoto, Japan) was used. The mobile phase consisted of 0.015 mol/L Na₂HPO₄:acetonitrile = 60:40, the detection wavelength was 290 nm, the column temperature was 30 °C, the loading speed was 1 mL/min, and the loading volume was 10 μ L.

3.5. Isolation and Identification of Major Metabolite

The isolation of the target metabolite was performed by semipreparative HPLC using an Elite SinoChrom ODS-BP (250 \times 10 mm \times 5 μ m, Dalian, China) consisting of a quaternary pump, a vacuum degasser, a variable wavelength detector, and an autosampler. The mobile phase consisted of acetonitrile and water in different percentages, and the proper fractions were collected.

ESI-MS and NMR analysis were performed under standard conditions.

3.6. Determination of the Standard Curve

Rabeprazole sulfide was accurately weighed, and a solution of 0.40 mg/mL was prepared, diluted step by step with methanol. Standard samples of 0.40, 0.30, 0.20, 0.15, 0.10, and 0.05 mg/mL were prepared and detected with HPLC, and a standard curve was drawn with rabeprazole sulfide concentration as the abscissa and peak area as the ordinate. This standard curve was used to calculate the conversion of rabeprazole sulfide. The total conversion rate was calculated according to the following equation:

$$\text{Conversion rate \%} = \frac{1 - \text{residue amount of rabeprazole sulfide}}{\text{Starting amount of rabeprazole sulfide}}$$

4. Conclusions and Discussion

By screening seven filamentous fungi, rabeprazole sulfide was the most efficiently decomposed into *O*-dimethyl rabeprazole sulfide by *Cunninghamella blakesleeana* 3.970, with a conversion rate of 72.4%. This is not a common biotransformation reaction type, with only few studies having suggested the *N*-demethylation [36,37] and *O*-dimethyl reactions [38,39].

The original aim of this study was to explore the possibility of whether these fungi could exhibit some oxidase activity so that the rabeprazole sulfide could be transformed into rabeprazole, i.e., to determine whether the thioether structure could be oxidized into the sulfoxide. Despite *Cunninghamella* species having exhibited various kinds of oxidation in previous works, no oxidation metabolites were identified in this research. Several reports have shown that *Absidia* and *Gibberella* species could exhibit oxidase activity as

their P450, but positive oxidation metabolites have yet to be generated. More importantly, *Caldariomyces fumago* was selected for its strong inner chloroperoxidase expression, which exhibited multiple oxidation types, such as epoxidation [40,41], hydroxylation [42–47], halogenation [48], etc. However, none of the above reactions were identified in this rabeprazole sulfide biotransformation.

Rabeprazole sulfide is actually not a natural substrate of the fungus, which was mentioned in the previous section on the influence of substrate concentration on the conversion rate. With the increase in substrate concentration, the conversion rate decreases (Figure 8), and a too-high concentration may produce some inhibition. It is speculated that the *O*-demethylation reaction of rabeprazole sulfide is not completed in one step. It may be that rabeprazole sulfide is first converted into one or several intermediate products and then further converted into *O*-demethyl rabeprazole sulfide.

Some microorganisms can transform drugs and other xenobiotic compounds in a manner similar to that in mammals, and the utilization of microbial systems as models for mimicking and predicting the metabolism of drugs in humans and animals has received considerable attention. Liu et al. reported that the main metabolic pathways of *Cunninghamella blakesleeana* to transform verapamil are *N*-dealkylation, *O*-demethylation, and sulfate coupling, and the *O*-demethylated metabolites of verapamil have the same potency as the parent drug [49]. Xie ZY et al. reported that approximately 92.5% of pantoprazole was metabolized to six metabolites by *Cunninghamella blakesleeana* AS 3.153, one of which was 4'-*O*-demethyl-pantoprazole thioether [30]. These studies did not deeply explore the mechanism of *O*-demethylation when *Cunninghamella blakesleeana* transformed the substrate. Therefore, it is of interest to further study the mechanism of the *O*-demethylation of *Cunninghamella blakesleeana* and the pharmacological or biological characteristics of these *O*-demethylated metabolites.

In addition, further investigation should be undertaken in the hunt for fungi that may oxidize thioether to sulfoxide. Meanwhile, other rational designs for the engineered enzyme to facilitate this reaction are also welcomed.

Supplementary Materials: The following are available online at <https://www.mdpi.com/article/10.3390/catal13010015/s1>, Figure S1. Growth of *Cunninghamella blakesleeana* 3.970 in 4 different transformation media. Figure S2. HPLC detection results of *Cunninghamella blakesleeana* 3.970 in 4 different transformation media. Figure S3. HPLC detection results of rabeprazole sulfide and its metabolites. Figure S4. HPLC detection results of rabeprazole sulfide metabolites for MS and NMR analysis. Figure S5. MS(ESI) m/z [M+H]⁺ diagram for the metabolite. Figure S6. MS(ESI) m/z [M+H][−] diagram for the metabolite. Figure S7. ¹H NMR diagram for the *O*-demethyl rabeprazole sulfide. Figure S8. ¹³C NMR diagram for the *O*-demethyl rabeprazole sulfide. Figure S9. ¹H NOESY diagram for the *O*-demethyl rabeprazole sulfide.

Author Contributions: M.S. (data curation, investigation); H.Z. (investigation, methodology); J.W. (rabeprazole and its sulfide preparation); W.X. (Weizhuo Xu) and W.X. (Wei Xu) (resources, supervision, writing—review and editing). All authors have read and agreed to the published version of the manuscript.

Funding: This research received no external funding.

Data Availability Statement: Data are available upon reasonable request.

Conflicts of Interest: The authors declare no conflict of interest.

References

1. FDA. Approval for Aciphex (Rabeprazole Sodium) Tablets. 2002. Available online: https://www.accessdata.fda.gov/drugsatfda_docs/nda/2002/021456_aciphex.cfm (accessed on 25 April 2003).
2. Duan, Z.; Wang, Y.; Zhang, L.; Cao, X.; Fu, L.; Li, Z.; Zhang, J. An application of continuous flow microreactor in the synthesis and extraction of rabeprazole. *Int. J. Chem. React. Eng.* **2021**, *19*, 287–294. [CrossRef]
3. Nishiguchi, S.; Izumi, T.; Kouno, T.; Sukegawa, J.; Ilies, L.; Nakamura, E. Synthesis of Esomeprazole and Related Proton Pump Inhibitors through Iron-Catalyzed Enantioselective Sulfoxidation. *ACS Catal.* **2018**, *8*, 9738–9743. [CrossRef]

4. Lu, C.; Jia, Y.; Song, Y.; Li, X.; Sun, Y.; Zhao, J.; Wang, S.; Shi, L.; Wen, A.; Ding, L. Application of a liquid chromatographic/tandem mass spectrometric method to a urinary excretion study of rabeprazole and two of its metabolites in healthy human urine. *J. Chromatogr. B* **2015**, *988*, 75–80. [[CrossRef](#)] [[PubMed](#)]
5. Zannikos, P.N.; Doose, D.R.; Leitz, G.J.; Rusch, S.; Gonzalez, M.D.; Solanki, B.; Haddad, I.; Mulberg, A.E. Pharmacokinetics and Tolerability of Rabeprazole in Children 1 to 11 Years Old with Gastroesophageal Reflux Disease. *J. Pediatr. Gastroenterol. Nutr.* **2011**, *52*, 691–701. [[CrossRef](#)] [[PubMed](#)]
6. Ren, S.; Park, M.-J.; Kim, A.; Lee, B.-J. In vitro metabolic stability of moisture-sensitive rabeprazole in human liver microsomes and its modulation by pharmaceutical excipients. *Arch. Pharmacol. Res.* **2008**, *31*, 406–413. [[CrossRef](#)]
7. Miura, M.; Satoh, S.; Tada, H.; Habuchi, T.; Suzuki, T. Stereoselective metabolism of rabeprazole-thioether to rabeprazole by human liver microsomes. *Eur. J. Clin. Pharmacol.* **2005**, *62*, 113–117. [[CrossRef](#)]
8. Sharara, A.I. Rabeprazole: The role of proton pump inhibitors in *Helicobacter pylori* eradication. *Expert Rev. Anti-Infect. Ther.* **2005**, *3*, 863–870. [[CrossRef](#)]
9. Lun, J.; Ma, S.; Xue, M.; Zhao, P.; Song, Y.; Guo, X. Simultaneous enantiomeric analysis of five proton-pump inhibitors in soil and sediment using a modified QuEChERS method and chiral high performance liquid chromatography coupled with tandem mass spectrometry. *Microchem. J.* **2020**, *160*, 105625. [[CrossRef](#)]
10. Marelli, S.; Pace, F. Rabeprazole for the treatment of acid-related disorders. *Expert Rev. Gastroenterol. Hepatol.* **2012**, *6*, 423–435. [[CrossRef](#)]
11. Yousuf, M.; Jamil, W.; Mammadova, M.Y.A.K. Microbial Bioconversion: A Regio-specific Method for Novel Drug Design and Toxicological Study of Metabolites. *Curr. Pharm. Biotechnol.* **2019**, *20*, 1156–1162. [[CrossRef](#)]
12. Asha, S.; Vidyavathi, M. *Cunninghamella*—A microbial model for drug metabolism studies—A review. *Biotechnol. Adv.* **2009**, *27*, 16–29. [[CrossRef](#)]
13. Murphy, C.D. Drug metabolism in microorganisms. *Biotechnol. Lett.* **2015**, *37*, 19–28. [[CrossRef](#)]
14. Keum, Y.-S.; Lee, Y.-H.; Kim, J.-H. Metabolism of methoxychlor by *Cunninghamella elegans* ATCC36112. *J. Agric Food Chem.* **2009**, *57*, 7931–7937. [[CrossRef](#)]
15. Choudhary, M.I.; Khan, N.T.; Musharraf, S.G.; Anjum, S.; Rahman, A.U. Biotransformation of adrenosterone by filamentous fungus, *Cunninghamella elegans*. *Steroids* **2007**, *72*, 923–929. [[CrossRef](#)]
16. Hanson, R.L.; Matson, J.A.; Brzozowski, D.B.; LaPorte, T.L.; Springer, D.M.; Patel, R.N. Hydroxylation of Mutilin by *Streptomyces griseus* and *Cunninghamella echinulata*. *Org. Process Res. Dev.* **2002**, *6*, 482–487. [[CrossRef](#)]
17. Ibrahim, A.; Khalifa, S.I.; Khafagi, I.; Youssef, D.T.; Khan, S.; Mesbah, M.; Khan, I. Microbial Metabolism of Biologically Active Secondary Metabolites from *Nerium oleander* L. *Chem. Pharm. Bull.* **2008**, *56*, 1253–1258. [[CrossRef](#)]
18. Kouzi, S.A.; Chatterjee, P.; Pezzuto, J.M.; Hamann, M.T. Microbial Transformations of the Antimelanoma Agent Betulinic Acid. *J. Nat. Prod.* **2000**, *63*, 1653–1657. [[CrossRef](#)]
19. Ning, L.; Zhan, J.; Qu, G.; Zhong, L.; Guo, H.; Bi, K.; Guo, D. Biotransformation of triptolide by *Cunninghamella blakesleana*. *Tetrahedron* **2003**, *59*, 4209–4213. [[CrossRef](#)]
20. Zhang, D.; Evans, F.E.; Freeman, J.P.; Duhart, B.; Cerniglia, C.E. Biotransformation of amitriptyline by *Cunninghamella elegans*. *Drug Metab. Dispos.* **1995**, *23*, 1417–1425.
21. Wu, Y.; Lu, Y.; Yi, Y.; Wang, A.; Wang, W.; Yang, M.; Fan, B.; Chen, G. Biotransformation of asiatic acid by *Cunninghamella echinulata* and *Circinella muscae* to discover anti-neuroinflammatory derivatives. *Nat. Prod. Res.* **2022**, *36*, 1–6. [[CrossRef](#)]
22. Khan, M.F.; Murphy, C.D. Cytochrome P450 5208A3 is a promiscuous xenobiotic biotransforming enzyme in *Cunninghamella elegans*. *Enzym. Microb. Technol.* **2022**, *161*, 110102. [[CrossRef](#)] [[PubMed](#)]
23. Bai, Y.; Zhao, Y.; Gao, X.; Zhang, D.; Ma, Y.; Yang, L.; Sun, P. A Novel Antimalarial Metabolite in Erythrocyte from the Hydroxylation of Dihydroartemisinin by *Cunninghamella elegans*. *Front. Chem.* **2022**, *10*, 850133. [[CrossRef](#)] [[PubMed](#)]
24. Sousa, I.P.; de SousaTeixeira, M.V.; Freitas, J.A.; Ferreira, A.G.; Pires, L.M.; Santos, R.A.; Heleno, V.C.G.; Furtado, N.A.J.C. Production of More Potent Anti- *Candida* Labdane Diterpenes by Biotransformation Using *Cunninghamella elegans*. *Chem. Biodivers.* **2022**, *19*, e202100757. [[CrossRef](#)] [[PubMed](#)]
25. Barrero, A.F.; Oltra, J.E.; Raslan, A.D.S.; Saúde, D.A. Microbial Transformation of Sesquiterpene Lactones by the Fungi *Cunninghamella echinulata* and *Rhizopus oryzae*. *J. Nat. Prod.* **1999**, *62*, 726–729. [[CrossRef](#)] [[PubMed](#)]
26. Zhang, D.; Hansen, E.B., Jr.; Deck, J.; Heinze, T.M.; Henderson, A.; Korfmacher, W.A.; Cerniglia, C.E. Fungal transformations of antihistamines: Metabolism of cyproheptadine hydrochloride by *Cunninghamella elegans*. *Xenobiotica* **1997**, *27*, 301–315. [[CrossRef](#)]
27. Zhou, L.; Xu, W.; Chen, Y.; Zhao, J.; Yu, N.; Fu, B.; You, S. Stereoselective epoxidation of curcumol and curdione by *Cunninghamella elegans* AS 3.2028. *Catal. Commun.* **2012**, *28*, 191–195. [[CrossRef](#)]
28. Grafinger, K.E.; Wilke, A.; König, S.; Weinmann, W. Investigating the ability of the microbial model *Cunninghamella elegans* for the metabolism of synthetic tryptamines. *Drug Test. Anal.* **2018**, *11*, 721–729. [[CrossRef](#)]
29. Nykodemová, J.; Šuláková, A.; Palivec, P.; Češková, H.; Rimpelová, S.; Šichová, K.; Leonhardt, T.; Jurásek, B.; Hájková, K.; Páleníček, T.; et al. 2C-B-Fly-NBOMe Metabolites in Rat Urine, Human Liver Microsomes and *C. elegans*: Confirmation with Synthesized Analytical Standards. *Metabolites* **2021**, *11*, 775. [[CrossRef](#)]
30. Xie, Z.Y.; Huang, H.H.; Zhong, D.F. Biotransformation of pantoprazole by the fungus *Cunninghamella blakesleana*. *Xenobiotica* **2005**, *35*, 467–477. [[CrossRef](#)]

31. Sutherland, J.B.; Freeman, J.P.; Heinze, T.M.; Moody, J.D.; Parshikov, I.A.; Williams, A.J.; Zhang, D. Oxidation of phenothiazine and phenoxazine by *Cunninghamella elegans*. *Xenobiotica* **2001**, *31*, 799–809. [[CrossRef](#)]
32. Zhang, D.; Freeman, J.P.; Sutherland, J.B.; Walker, A.E.; Yang, Y.; Cerniglia, C.E. Biotransformation of chlorpromazine and methdilazine by *Cunninghamella elegans*. *Appl. Environ. Microbiol.* **1996**, *62*, 798–803. [[CrossRef](#)]
33. Bachmann, F.; zu Schwabedissen, H.E.M.; Duthaler, U.; Krähenbühl, S. Cytochrome P450 1A2 is the most important enzyme for hepatic metabolism of the metamizole metabolite 4-methylaminoantipyrine. *Br. J. Clin. Pharmacol.* **2021**, *88*, 1885–1896. [[CrossRef](#)]
34. Ren, H.; Dhanaraj, P.; Enoch, I.V.; Paulraj, M.S.; Paulraj, M.S. Synthesis and Biological Evaluation of 4-Aminoantipyrine Analogues. *Med. Chem.* **2022**, *18*, 26–35. [[CrossRef](#)]
35. Eliwa, D.; Albadry, M.A.; Ibrahim AR, S.; Kabbash, A.; Meepagala, K.; Khan, I.A.; El-Aasr, M.; Ross, S.A. Biotransformation of papaverine and in silico docking studies of the metabolites on human phosphodiesterase 10a. *Phytochemistry* **2021**, *183*, 112598. [[CrossRef](#)]
36. Yang, W.; Jiang, T.; Acosta, D.; Davis, P.J. Microbial models of mammalian metabolism: Involvement of cytochrome P450 in the N-demethylation of N-methylcarbazole by *Cunninghamella echinulata*. *Xenobiotica* **1993**, *23*, 973–982. [[CrossRef](#)]
37. Hansen, E.B., Jr.; Cho, B.P.; Korfmacher, W.A.; Cerniglia, C.E. Fungal transformations of antihistamines: Metabolism of brompheniramine, chlorpheniramine, and pheniramine to N-oxide and N-demethylated metabolites by the fungus *Cunninghamella elegans*. *Xenobiotica* **1995**, *25*, 1081–1092. [[CrossRef](#)]
38. Fan, H.X.; Zhou, Z.Q.; Peng, J.; Wu, B.J.; Chen, H.R.; Bao, X.F.; Mu, Z.Q.; Jiao, W.H.; Yao, X.S.; Gao, H. A microbial model of mammalian metabolism: Biotransformation of 4,5-dimethoxyl-canthin-6-one using *Cunninghamella blakesleeana* CGMCC 3.970. *Xenobiotica* **2017**, *47*, 284–289. [[CrossRef](#)]
39. Ibrahim, A.-R.S.; Galal, A.M.; Ahmed, M.S.; Mossa, G.S. O-Demethylation and Sulfation of 7-Methoxylated Flavanones by *Cunninghamella elegans*. *Chem. Pharm. Bull.* **2003**, *51*, 203–206. [[CrossRef](#)]
40. Liu, Y.; Wang, Y.; Jiang, Y.; Hu, M.; Li, S.; Zhai, Q. Biocatalytic synthesis of C3 chiral building blocks by chloroperoxidase-catalyzed enantioselective halo-hydroxylation and epoxidation in the presence of ionic liquids. *Biotechnol. Prog.* **2015**, *31*, 724–729. [[CrossRef](#)]
41. Morozov, A.N.; Chatfield, D.C. Chloroperoxidase-catalyzed epoxidation of cis-beta-methylstyrene: Distal pocket flexibility tunes catalytic reactivity. *J. Phys. Chem. B* **2012**, *116*, 12905–12914. [[CrossRef](#)]
42. de Hoog, H.M.; Nallani, M.; Cornelissen, J.J.L.M.; Rowan, A.E.; Nolte, R.J.M.; Arends, I.W.C.E. Biocatalytic oxidation by chloroperoxidase from *Caldariomyces fumago* in polymersome nanoreactors. *Org. Biomol. Chem.* **2009**, *7*, 4604–4610. [[CrossRef](#)] [[PubMed](#)]
43. Kellner, H.; Pecyna, M.J.; Buchhaupt, M.; Ullrich, R.; Hofrichter, M. Draft Genome Sequence of the Chloroperoxidase-Producing Fungus *Caldariomyces fumago* Woronichin DSM1256. *Genome Announc.* **2016**, *4*, e00774-16. [[CrossRef](#)] [[PubMed](#)]
44. Dong, X.; Li, H.; Jiang, Y.; Hu, M.; Li, S.; Zhai, Q. Rapid and efficient degradation of bisphenol A by chloroperoxidase from *Caldariomyces fumago*: Product analysis and ecotoxicity evaluation of the degraded solution. *Biotechnol. Lett.* **2016**, *38*, 1483–1491. [[CrossRef](#)] [[PubMed](#)]
45. Buchhaupt, M.; Hüttmann, S.; Sachs, C.C.; Bormann, S.; Hannappel, A.; Schrader, J. *Caldariomyces fumago* DSM1256 Contains Two Chloroperoxidase Genes, Both Encoding Secreted and Active Enzymes. *J. Mol. Microbiol. Biotechnol.* **2015**, *25*, 237–243. [[CrossRef](#)] [[PubMed](#)]
46. Buchhaupt, M.; Hüttmann, S.; Schrader, J. White Mutants of Chloroperoxidase-Secreting *Caldariomyces fumago* as Superior Production Strains, Revealing an Interaction between Pigmentation and Enzyme Secretion. *Appl. Environ. Microbiol.* **2012**, *78*, 5923–5925. [[CrossRef](#)]
47. Buchhaupt, M.; Ehrich, K.; Hüttmann, S.; Guder, J.; Schrader, J. Over-expression of chloroperoxidase in *Caldariomyces fumago*. *Biotechnol. Lett.* **2011**, *33*, 2225–2231. [[CrossRef](#)]
48. Höfler, G.T.; But, A.; Hollmann, F. Haloperoxidases as catalysts in organic synthesis. *Org. Biomol. Chem.* **2019**, *17*, 9267–9274. [[CrossRef](#)]
49. Sun, L.; Huang, H.-H.; Liu, L.; Zhong, D.-F. Transformation of Verapamil by *Cunninghamella blakesleeana*. *Appl. Environ. Microbiol.* **2004**, *70*, 2722–2727. [[CrossRef](#)]

Disclaimer/Publisher's Note: The statements, opinions and data contained in all publications are solely those of the individual author(s) and contributor(s) and not of MDPI and/or the editor(s). MDPI and/or the editor(s) disclaim responsibility for any injury to people or property resulting from any ideas, methods, instructions or products referred to in the content.